Supporting information

Vapor Phase Synthesis of Single-Crystalline Ag Nanowires and Single-Nanowire Surface-Enhanced Raman Scattering

Paritosh Mohanty,[†] Ilsun Yoon,[†] Taejoon Kang,[†] Kwanyong Seo,[†] Kumar S. K. Varadwaj,[†] Wonjun Choi,[‡] Q-Han Park,[‡] Jae Pyung Ahn,[§] Yung Doug Suh,[‖] Hyotcherl Ihee,[†] and Bongsoo Kim[†,*]

[†]Department of Chemistry, KAIST, Daejeon 305-701, Korea,

[‡]Department of Physics, Korea University, Seoul 136-701, Korea,

[§]Nano-Material Research Center, KIST, Seoul 136-791, Korea,

[‖]Division of Advanced Chemical Materials, KRICT, Daejeon 305-600, Korea.

* To whom correspondence should be addressed. Email: bongsoo@kaist.ac.kr

Experimental details

Ag NWs Synthesis. In a typical synthesis, 0.2 g of Ag_2O precursor powder (Sigma-Aldrich; purity = 99.996 %) was placed in an alumina boat at the middle of a 1 inch diameter horizontal quartz tube furnace. The NWs were grown at about 3-4 cm down-stream from the precursor on a Si substrate. At high temperature (T_1 = 900 − 1000 °C) the precursor vapor was carried downstream by the flow of 500 sccm of argon gas at a pressure of 5 to 10 Torr to a lower temperature zone (T_2 = 500 °C), where it is reduced to metallic Ag.

X-ray Diffraction. The XRD pattern of as grown Ag NWs was recorded using a Rigaku D/max-RC (12 kW) diffractometer with the Cu Kα radiation ($λ$ = 1.5406 Å) at a scanning rate of 3° per minute in 2θ ranging from 30° to 80°. Four distinguished peaks of Figure S1 are indexed perfectly to the face centered cubic (fcc) phase of Ag. This pattern was very close to the reported data (JCPDS File no. 04-0783).
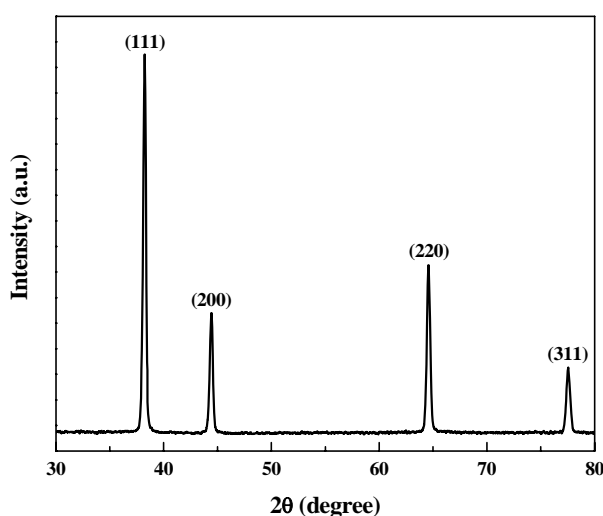

Figure S1. XRD pattern of Ag NWs.

X-ray Energy-dispersive Spectrometry. For TEM investigation, a drop of ethanolic suspension of Ag NWs was placed on a holey carbon-coated copper grid and dried. TEM and electron diffraction studies were taken on TECNAI F20 and JEOL JEM-2100F microscope operated at 200 kV. Chemical compositions of the NW were studied by X-ray Energy-dispersive spectrometry (EDS) attached to the TEM. Compositional maps and spectra for the Ag NW are shown in Figure S2. Only Ag peaks are seen except some peaks from copper and carbon which are due to the TEM grid. This confirms that the NW contains only Ag.
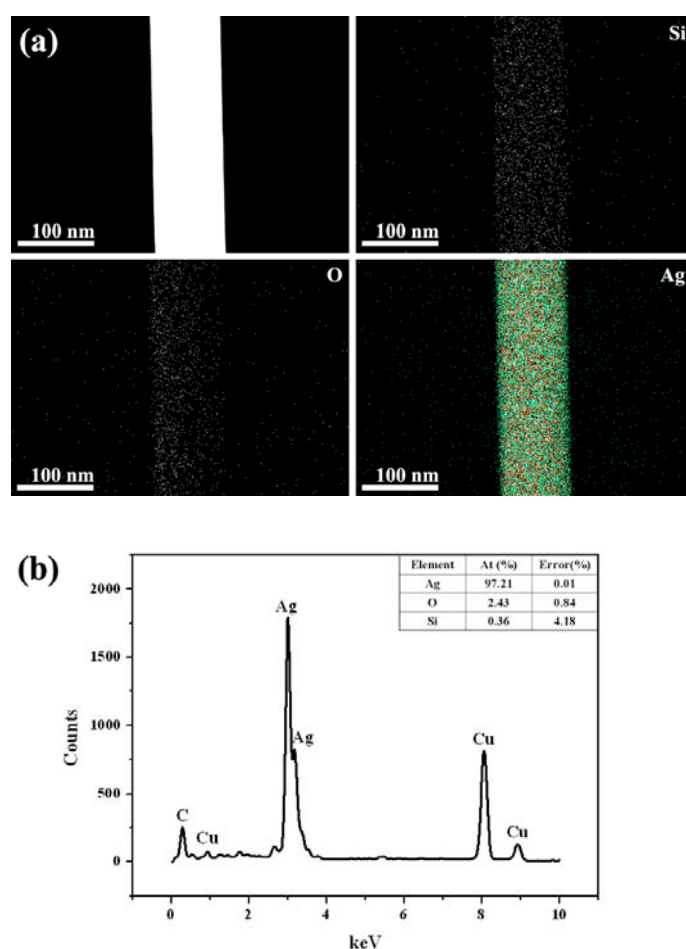

Figure S2. (a) EDS mapping for Ag, O, and Si (b) EDS spectrum of Ag NWs. The inset in (b) shows the atomic ratio of Ag, O, and Si on a Ag NW.

SERS measurement. Ag NWs for SERS measurement were prepared by dropping ethanolic solution of NWs onto a Si substrate. A drop of 10^{-2} M ethanolic solution of brilliant cresyl blue (BCB) was put and dried on a Si substrate. We searched for single NWs far from clots of BCB and minimized the affection of Raman spectrum of bulk BCB on SERS spectra of BCB adsorbed on Ag NWs.

Figure S3 shows the home-made microRaman system, which was based on an Olympus BX41 microscope.
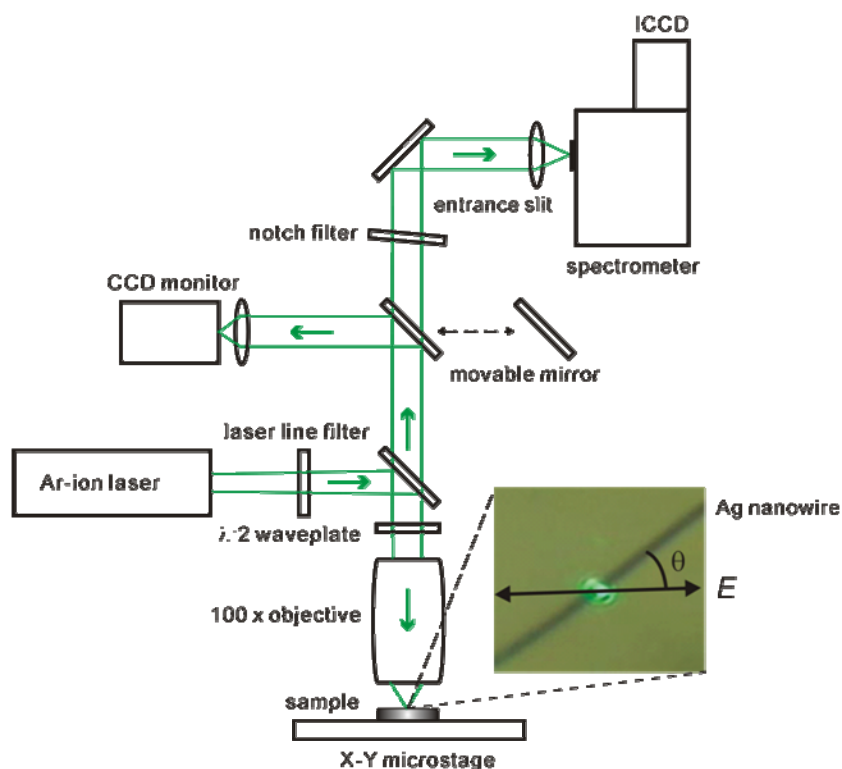

Figure S3. Micro-Raman system for the measurement of SERS of Ag NWs.

A 514.5 nm Ar-ion laser light with linear polarization was used as a Raman excitation source. A half-wave plate rotated the polarization direction of the incident laser light. The laser light was focused on a NW through an objective (Mitutoyo M PLAN APO 100 ×, NA 0.7). The backscattered light was collected through the same objective and directed to a

4

spectrometer with a 1200 groove/mm grating. The spectrometer was equipped with an intensified charge coupled device (ICCD, Andor iStar DH720) detector. The ICCD was thermoelectrically cooled and operated at -35 °C. A holographic notch filter was used to reject the 514.5 nm laser light.

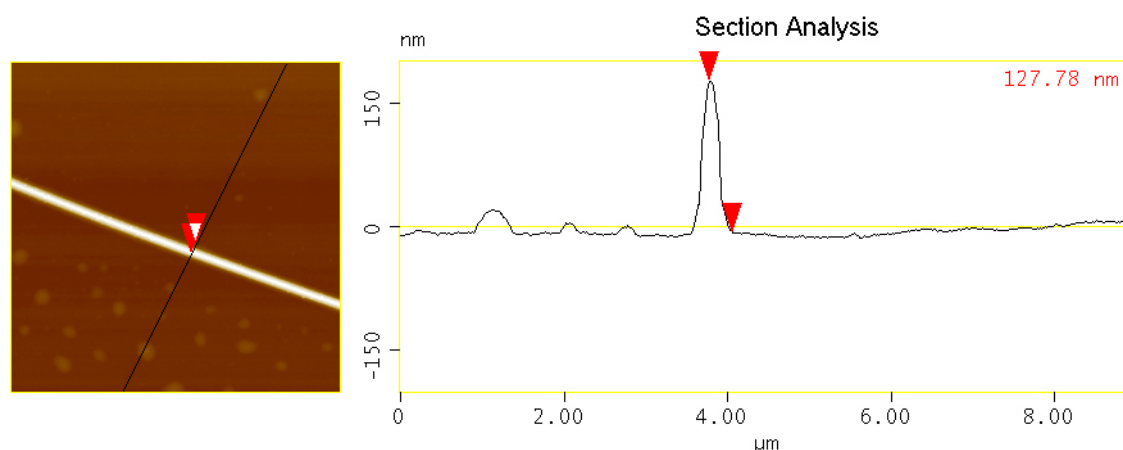**AFM image of a single Ag NW.**

Figure S4. The AFM image of a Ag NW on which we obtained SERS.

The image is obtained with Veeco bioscope AFM controlled by Nanoscope IV controller. This image confirms that the Ag NW is a separated single NW and not bundled NWs.

Polarized SERS signal. The center of the NW was translated to the green laser spot manually by a X-Y stage. The incident laser power was 0.8 mW and total data collection time for each spectrum was 30 seconds. SERS spectra were taken at the same position with different polarization directions with respect to the NW axis. θ is the angle between the NW axis and the polarization direction. As Figure S5 shows, weak Raman signals were observed when $\theta = 10°$. The Raman signals were maximized when θ approached to 90°. The polar plot of integrated SERS intensities is shown at Figure 2(d). θ was changed from 10° to 350° by

increments of 20°. The blue and magenta lines represent the best fits of Raman bands to a a

$e^{-\theta}\cos^2(\theta)$ function. An exponential decay function was included to correct the signal

attenuation by the bleaching effect. The goodness-of-fit values, R^2, of the each line were 0.98
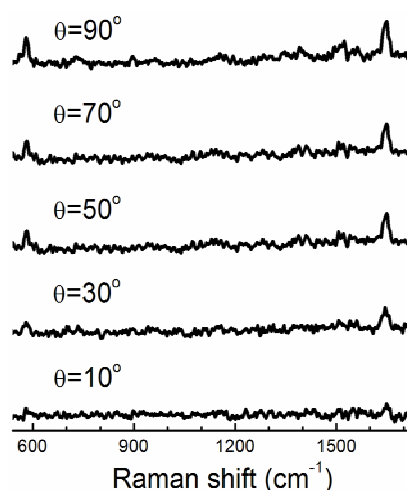
and 0.93 respectively.

Figure S5. SERS spectra of BCB adsorbed on an individual Ag NW at different polarization
directions.

We tried to observe enhanced Raman signals at the tip of NWs with perpendicular and

parallel polarization directions. As Figure S6 shows, no enhancement and no lighting rod

effect were observed at the end edge (point P2) of the NW with comparison to SERS signal

measured at the center (point P1) of the NW. In this measurement, the Ar-ion laser power was

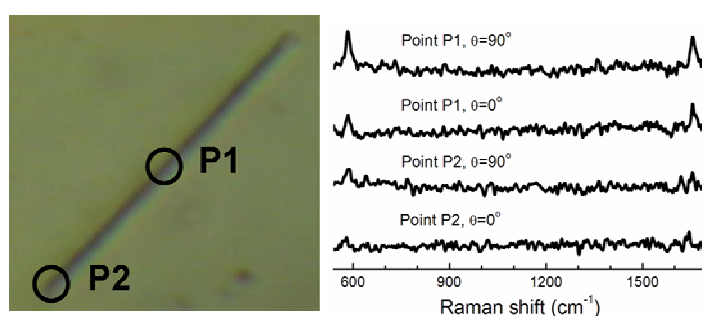0.3 mW and the data collection time was 30 seconds.

Figure S6. SERS spectra of BCB adsorbed to two different points of P1 (the center) and P2

(the end edge) of a Ag NW with parallel and perpendicular polarization direction to the NW axis.
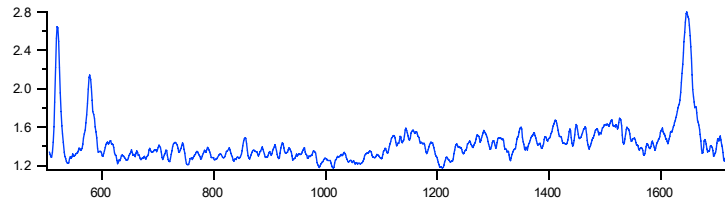
Raman signal from the bare Si plate.

Figure S7. Original SERS spectrum of Figure 2(b) top spectrum. The Si Raman peak is seen at 520 cm^{-1}, and is deleted in Figure 2(b) for the ease of comparison.

Estimation of enhancement factor We assume that BCB dye is evenly distributed around the Ag NWs and Si plate and the diameter of Ag NW is 100 nm. The laser-illuminated area on a Si plate has 7.5 times larger effective area than that on a Ag NW, when the laser spot has a diameter of 1 micron.

	Signal intensity from Integrated Area	Standard deviation of Noise
Si	4×10^5	2×10^5
Ag NW (parallel polarization)	1.0×10^6	2×10^5
Ag NW (perpendicular polarization)	4.2×10^6	2×10^5

The SERS signal for a Ag NW when the light is perpendicularly polarized is 10 times larger than the Raman signal of BCB on a Si plate. When the effective area is considered, we conclude that the SERS signal of the Ag NW is about 75 times larger than the Raman signal on Si. Note that this number could have been underestimated because the noise is rather large compared to the Raman signal on Si. We plan to replace the ICCD to a much lower noise

EMCCD, which would reduce the noise significantly.

FDTD calculation. FDTD calculations were performed to investigate the local electrical field near the NW at the excitation wavelength of 514.5 nm.
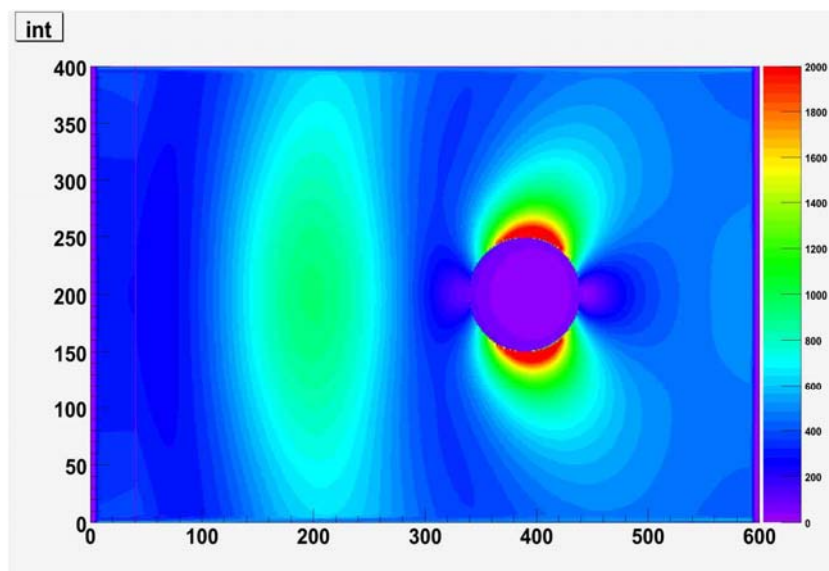

Figure S8. 2-dimensional crosscut of 3-dimensional FDTD result. Ag NW is seen in the right. The color scale shows the intensity of the electric field

In our FDTD calculation, we have executed a fully 3-dimensional FDTD and excited NW locally by using a Gaussian beam with 500 nm FWHM (The experimentally estimated beam size). Thus the excited field was limited in only a localized section of the NW. The full size enlarged Figure S8 shows this more clearly. The color scale bar is not in a normalized fashion, and the incident Gaussian beam has a maximum intensity of unit 500 in the color scale bar. Therefore, the local maximum of EM field is enhanced by about 6 - 7 fold compared to original laser field.

Short-axis cross-sections of the electrical field distribution around a NW with parallel and perpendicular incident polarization directions ($\theta = 0°$, $\theta = 90°$) are shown in Figure S9. Black circles are drawn to represent NWs. In these calculations, the diameter of the NW was set as 100 nm.

Strong electrical field is induced and localized near the NW when the polarization direction is perpendicular to the NW axis ($\theta = 90°$). The electrical field is not enhanced on the top and the bottom of the NW. When the polarization direction is parallel to the NW axis ($\theta = 0°$), the electrical field is not enhanced near the NW. In detail, $|E|^2_X$ and $|E|^2_Z$ components of the electrical field are localized and enhanced near the NW when the polarization is perpendicular to the NW axis. The $|E|^2_Y$ component is not localized and enhanced at this incident polarization. When the incident polarization direction is parallel to the NW, only $|E|^2_Y$ component is a little enhanced near the NW.
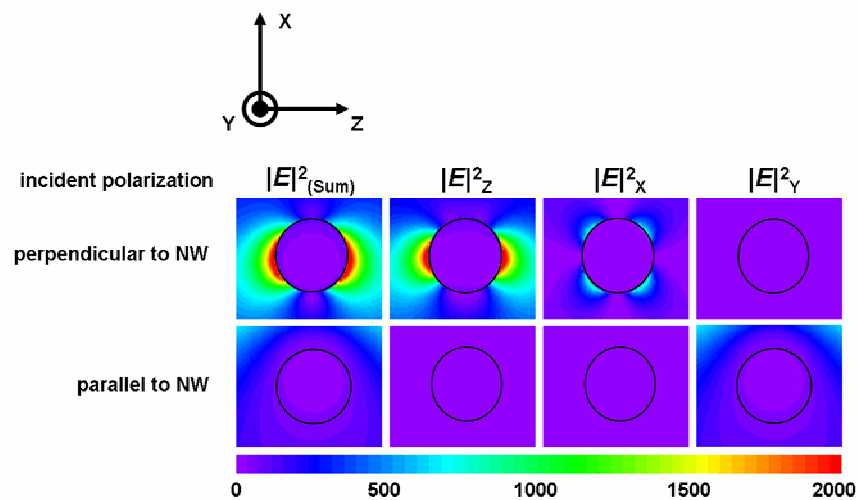

Figure S9. X, Y, and Z components of the electric field and its summation around the NW with perpendicular and parallel polarization directions to the NW calculated by FDTD. The 514.5 nm light is incident on the NW along the X direction with perpendicular (Z-axis directed) and parallel (Y-axis directed) polarization directions to the NW axis.